PROTEINS
STRUCTURE ■ FUNCTION ■ BIOINFORMATICS

STRUCTURE NOTE

Solution NMR structure of the ribosomal protein RP-L35Ae from *Pyrococcus furiosus*

David A. Snyder,[1,2] James M. Aramini,[2] Bomina Yu,[2] Yuanpeng J. Huang,[2] Rong Xiao,[2] John R. Cort,[3] Ritu Shastry,[2] Li-Chung Ma,[2] Jinfeng Liu,[4] Burkhard Rost,[4] Thomas B. Acton,[2] Michael A. Kennedy,[5] and Gaetano T. Montelione[2,6]*

[1] Department of Chemistry, College of Science and Health, William Paterson University, Wayne, New Jersey 07470

[2] Department of Molecular Biology and Biochemistry, Center for Advanced Biotechnology and Medicine, and The Northeast Structural Genomics Consortium, Rutgers, The State University of New Jersey, Piscataway, New Jersey 08854

[3] Biological Sciences Division, Pacific Northwest National Laboratory, and The Northeast Structural Genomics Consortium, Richland, Washington 99352

[4] Department of Biochemistry and Molecular Biophysics, Center for Computational Biology and Bioinformatics, and The Northeast Structural Genomics Consortium, Columbia University, New York, New York 10032

[5] Department of Chemistry and Biochemistry, and The Northeast Structural Genomics Consortium, Miami University, Oxford, Ohio 45056

[6] Department of Biochemistry, Robert Wood Johnson Medical School, University of Medicine and Dentistry of New Jersey, Piscataway, New Jersey 08854

ABSTRACT

The ribosome consists of small and large subunits each composed of dozens of proteins and RNA molecules. However, the functions of many of the individual protomers within the ribosome are still unknown. In this article, we describe the solution NMR structure of the ribosomal protein RP-L35Ae from the archaeon *Pyrococcus furiosus*. RP-L35Ae is buried within the large subunit of the ribosome and belongs to Pfam protein domain family PF01247, which is highly conserved in eukaryotes, present in a few archaeal genomes, but absent in bacteria. The protein adopts a six-stranded anti-parallel β-barrel analogous to the "tRNA binding motif" fold. The structure of the *P. furiosus* RP-L35Ae presented in this article constitutes the first structural representative from this protein domain family.

Proteins 2012; 00:00–00.

Key words: ribosomal protein; L35Ae; PF01247; tRNA binding; EF-Tu/eEF-1A; solution NMR; structural genomics

INTRODUCTION

Ribosomes are ubiquitous macromolecular complexes composed of two subunits, each of which are made up of several proteins and RNA molecules, hundreds of nucleotides in length. Ribosomes are responsible for protein synthesis in all living cells. The catalytic core of ribosomes—where the information encoded on mRNA is translated, tRNAs are bound, and peptide bonds are formed—is highly conserved throughout evolution. Peripheral activities of the ribosome are less conserved, reflecting differences in the mechanisms of protein

Additional Supporting Information may be found in the online version of this article.
Grant sponsor: National Institute of General Medical Sciences Protein Structure Initiative (PSI); Grant numbers: U54-GM074958 and U54-GM094597 (Gaetano T. Montelione).
Partial support was also provided to David A. Snyder as Assigned Release Time from William Paterson University.
*Correspondence to: Gaetano T. Montelione, CABM, Rutgers University, 679 Hoes Lane, Piscataway, NJ 08854. E-mail: guy@cabm.rutgers.edu
Received 7 February 2012; Accepted 3 March 2012
Published online 16 March 2012 in Wiley Online Library (wileyonlinelibrary.com).
DOI: 10.1002/prot.24071

synthesis. Eukaryotic ribosomes are substantially larger and more complex than those of eubacteria. Homologous eukaryotic ribosomal proteins often have extra protein fragments and the RNA molecules have expansion segments, which, together with the ~25 unique eukaryotic ribosomal proteins, contribute to the observed 40% increase in size.[1]

The RP-L35Ae domain family includes ribosomal proteins known to be buried within the large subunit of the ribosome[2] and to bind both initiator and elongator tRNA molecules.[3] Eukaryotic homologs also appear to function extra-ribosomally as inhibitors of apoptosis[4] and are over-expressed in certain cancer cell lines, which contribute to resistance to chemotherapeutic agents.[5] This contrasts with many other proteins associated with translation that function extra-ribosomally as promoters of apoptosis.[6] However, the precise roles of RP-L35Ae proteins in the mechanism of translation and their function(s) outside the ribosome are not known.

RP-L35Ae proteins belong to the highly conserved Pfam PF01247 protein domain family[7] [Fig. 1(a)]. Absent in bacterial genomes, homologs of RP-L35Ae are found in only four classes of archaea (www.orthology.org). The crystal structure of the large ribosomal subunit of *Haloarcula marismortui* lacks an RP-L35Ae homolog,[8] further demonstrating that this ribosomal protein is not required in at least some archaeal ribosomes. In fact, the ribosomes of many "crown" euryarchaeotes lack homologs for up to 10 eukaryotic ribosomal proteins, apparently a result of "reductive evolution." In most cases, the collection of archaea lacking a homolog of a particular eukaryotic ribosomal protein form a monophyletic group (clade), however, the organisms lacking RP-L35Ae homologs do not constitute a single clade.[9] Studies of isolated ribosomal proteins play a critical role in elucidating the structure of ribosomes as a whole and can provide valuable insights into the extra-ribosomal functions of these proteins as well as into the mechanisms of ribosomal reductive evolution.

In this article, we present the solution NMR structure of RP-L35Ae from *Pyrococcus furiosus*. This protein was selected for three-dimensional structure determination by the Northeast Structural Genomics Consortium (NESG; http://www.nesg.org) as part of the NIH Protein Structure Initiative on structural coverage of large, broadly conserved protein domain families. RP-L35Ae is an 87-residue basic protein (UniProtKB/Swiss-Prot ID, RL35A_PYRFU; NESG ID, PfR48). When deposited and released in the PDB, its structure was the first structural representative of this important protein domain family.

MATERIALS AND METHODS

P. furiosus RP-L35Ae was cloned, expressed, and purified following standard NESG protocols.[10] Briefly, the *rpl35Ae* gene (UniProtKB/Swiss-Prot ID, RL35A_PYRFU; NESG ID, PfR48; hereafter referred to as RP-L35Ae) from *P. furiosus* was amplified from genomic DNA and cloned into the pET21_NESG vector (Novagen) in frame with a C-terminal affinity tag (LEHHHHHH), transformed into *E. coli* BL21(DE3) pMGK cells, and expressed overnight at 17°C in MJ9 minimal media.[11] Isotopically enriched samples were produced using *U*-$(^{15}NH_4)_2SO_4$ and *U*-^{13}C-glucose as the sole nitrogen and carbon sources. Proteins were purified using an ÄKTAxpress system (GE Healthcare) with a two-step protocol consisting of IMAC (HisTRAP HP) and gel filtration (HiLoad 26/60 Superdex 75) chromatography. Final yields of 6 mg of [*U*-^{13}C,^{15}N]-RP-L35Ae and 25 mg of [*U*-5%-^{13}C,100%-^{15}N]-RP-L35Ae were obtained per liter of cell culture and concentrated to 0.3–1.1 m*M* in 90% H_2O/10% ^2H_2O, 20 m*M* MES, 100 m*M* NaCl, 5 m*M* $CaCl_2$, 10 m*M* DTT, 50 μ*M* DSS, pH 6.5. The pET expression vector for *P. furiosus* RP-L35Ae (NESG PfR48-21.1), has been deposited in the PSI Materials Repository (http://psimr.asu.edu/).

All NMR data for resonance assignment and structure determination were collected at 293 K on Varian INOVA 600, 750, and 800 MHz and Varian UNITY 600 MHz spectrometers equipped with 5 mm HCN probes, processed with NMRPipe 2.1[12] and visualized using SPARKY 3.106.[13] All spectra were referenced to internal DSS. Complete ^{1}H, ^{13}C, and ^{15}N resonance assignments for RP-L35Ae were determined using conventional triple resonance NMR methods. Backbone resonance assignments were made by AutoAssign 1.9[14] using peak lists for 2D ^{1}H–^{15}N HSQC and 3D HNCO, CBCA(CO)NH, and HNCACB spectra. Side chain assignment was completed manually using 3D HBHA(CO)NH, HCCH-COSY, (H)CCH-TOCSY, and CC(CO)NH-TOCSY experiments. Stereospecific isopropyl methyl resonance assignments for all Val and Leu residues were determined from characteristic cross-peak fine structures in high resolution 2D ^{1}H–^{13}C HSQC spectra of [*U*-5%-^{13}C,100%-^{15}N]-RP-L35Ae.[15] Resonance assignments were validated using the Assignment Validation Suite (AVS) software package.[16] Three-bond $^3J(H^N\text{-}H^\alpha)$ scalar couplings were determined using the 3D HNHA experiment.[17]

The solution NMR structure of RP-L35Ae was calculated using CYANA 3.0,[18,19] supplied with peak intensities from the following NOESY spectra (with τ_m = 140 ms and in 10% ^2H_2O, unless otherwise specified): 3D ^{15}N-edited NOESY (τ_m = 100 ms), 3D ^{13}C-edited aliphatic NOESY, 3D ^{13}C-edited aliphatic NOESY (in 100% ^2H_2O), and 3D ^{13}C-edited aromatic NOESY, together with broad dihedral angle constraints computed by TALOS+[20] (ϕ, $\psi \pm 30°$) for ordered residues with confidence scores of 10, and hydrogen bond constraints. The 20 structures with lowest target function out of 100 calculated in the final cycle were further refined by restrained molecular dynamics in explicit water using CNS 1.3[21,22] and the PARAM19 force field, supplied

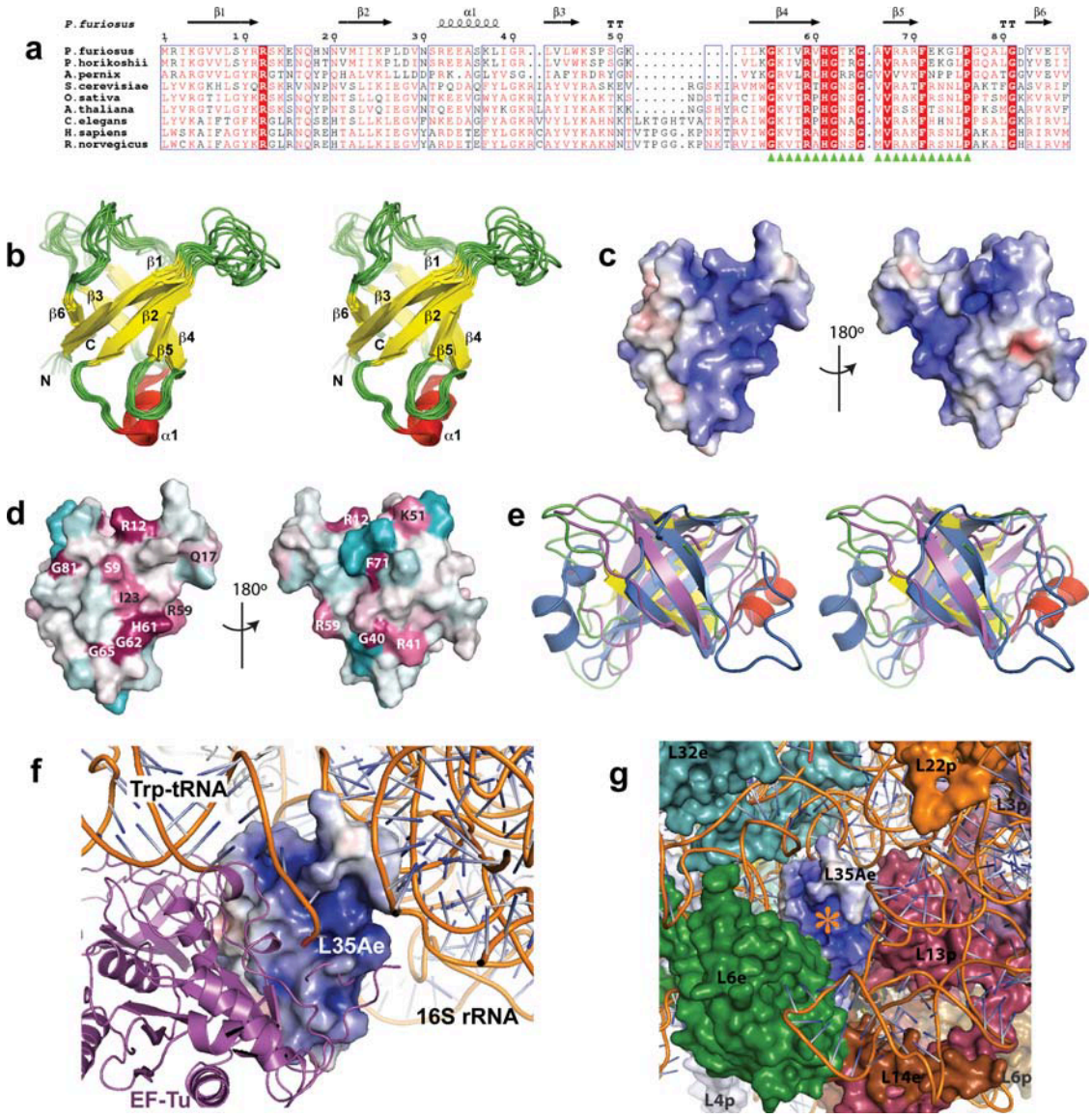

Figure 1

Solution NMR structure of RP-L35Ae from *Pyrococcus furiosus*. (**a**) Sequence alignment of representatives of the RP-L35Ae Pfam PF01247 protein domain family by ClustalW.[42] Only the region of the alignment corresponding to the *P. furiosus* protein is shown. The sequence for *Oryza sativa* was used to model the *Triticum aestivum* cryo-EM structure.[40] Boxed residues highlighted red or colored white represent residues that have 100% sequence identity or are conservatively substituted, respectively. The PROSITE[33] signature sequence, G[K/T][L/I/V/M]x[R/D]xHGxxGxVx[A/V/S]xFxxx[L/I]P, is indicated by green triangles. The secondary structure elements found in the NMR structure of *P. furiosus* RP-L35Ae are shown above the alignment. TT represents strict β-turns. (**b**) Stereo pair of the final ensemble of conformers from the solution NMR structure of *P. furiosus* RP-L35Ae with α-helices, β-strands, and loops colored red, yellow, and green, respectively. (**c**) Electrostatic surface potential[31] of RP-L35Ae. Fully saturated red and blue colors represent, respectively, negative and positive potentials of ±5 kT at an ionic strength of 0.2 *M*. (**d**) ConSurf[32] image showing the conserved residues in the entire Pfam PF01247 protein domain family with the degree of residue conservation ranging from highly conserved (magenta) to variable (cyan). Selected conserved residues are labeled. (**e**) Stereo pair of the least-squares superposition of EF-Tu/eEF-1A from *T. thermophilus* (purple, PDB ID 2XQD),[36] and Gar1 from *P. furiosus* (blue, PDB ID 3HAY)[43] onto RP-L35Ae (colored according to panel b). Only the structurally similar domains of EF-Tu/eEF-1A and Gar1 are shown. (**f**) Least-squares superposition of RP-L35Ae (electrostatic surface potential colored according to panel c) on an EF-Tu/eEF-1A -tRNA-ribosome ternary complex (PDB ID 2XQD).[36] EF-Tu/eEF-1A is shown in purple, the superimposed RP-L35Ae in blue, and the 16S ribosomal RNA and Trp-tRNA are shown in orange and yellow, respectively. (**g**) Least-squares superposition of RP-L35Ae (electrostatic surface potential colored according to panel c) on the L35Ae subunit in the cryo-EM structure of the 80S ribosome from *T. aestivum* (PDB ID 3IZR, 3IZ9, 3IZ6, 3IZ7).[40] The ribosomal proteins are labeled according to the protein family. The proposed tRNA binding site is indicated by an orange asterisk. The 28S rRNA is shown in orange and blue. Figures were created by ESPript[44] and PyMOL (www.pymol.org).

with the final NOE-derived distance, TALOS+ dihedral angle, and hydrogen bond constraints. In this final stage of the structure determination, rotamer states of specific-ordered residues were constrained (χ_1, χ_2 $\pm 20^\circ$) based on MolProbity[23,24] and PROCHECK[25] analyses.

The final refined ensemble of 20 structures (excluding the four C-terminal unassigned histidines) was deposited into the Protein Data Bank (PDB ID 2LP6) and BioMagResDB (BMRB accession number 6173). Structural statistics and global structure quality factors, including Verify3D,[26] ProsaII,[27] PROCHECK,[25] and MolProbity[23,24] raw and statistical *Z*-scores were computed using the PSVS 1.4 software package.[28] The global goodness-of-fit of the final structure ensemble with the NOESY peak list data and resonance assignments was determined using the RPF analysis program.[29]

RESULTS AND DISCUSSION

The solution structure of RP-L35Ae reported in this article corresponds to the first structural representative from the Pfam PF01247 (Ribosomal_L35Ae) protein domain family.[7] The protein eluted from the gel-filtration column as a monomer during purification. The NMR structure consists of a six-stranded anti-parallel β-barrel with an additional α-helix between strands β2 and β3 of the barrel [Fig. 1(b)]. Several lines of spectroscopic evidence, analyzed automatically by AutoStructure[30] and manually validated, confirm the observed secondary structure and barrel topology of β1-β2-β5-β4-β3-β6. These include the chemical shift values, $^3J(H^N–H^\alpha)$ scalar coupling constants, and the observed pattern of sequential and medium range NOEs (Supporting Information Figure S1). Table I presents statistics that characterize the quality of the resulting i.e., RP-L35Ae structure. Similar structures and structure quality scores were obtained using AutoStructure[30] for automated NOESY spectral analysis.

Electrostatic surface potential[31] [Fig. 1(c)] and ConSurf[32] [Fig. 1(d)] images reveal that one face of the RP-L35Ae β-barrel is particularly positively charged and that the PROSITE[33] signature sequence for the RP-L35Ae family [Fig. 1(a)] lies alongside a very cationic pocket on this positively charged face. SCOP[34] and CATH[35] classify the RP-L35Ae structure to a fold/topology class including such tRNA binding domains as the β-barrel domains of EF-Tu/eEF-1A[36] and Gar1[37] [Fig. 1(e)]. Although, there is no significant sequence similarity between RP-L35Ae family members and other domains having the same β-barrel structure, a structural superimposition of RP-L35Ae into the structure of a ternary EF-Tu/eEF-1A—tRNA—ribosome complex[36] reveals that L35Ae and EF-Tu/eEF-1A may share a similar tRNA binding site [Fig. 1(f)]; in particular, when superimposed onto eEF-1A in this protein-tRNA complex, the basic face of RP-L35Ae is juxtaposed with the Trp-tRNA, indicating a tRNA-binding function for RP-L35Ae. This putative tRNA binding site of RP-L35Ae proteins is corroborated by its sequence conservation across the RP-L35Ae family. Other conserved surface patches on the RP-L35Ae β-barrel may be involved in binding other ribosomal proteins, as well as ribosomal

Table I
Summary of NMR and Structural Statistics[a]

	RP-L35Ae	
Completeness of resonance assignments[b]		
Backbone (%)	98.2	
Side chain (%)	90.9	
Aromatic (%)	100	
Stereospecific methyl (%)	84.2	
Conformationally restricting constraints[c]		
Distance constraints		
Total	1402	
Intra-residue ($i = j$)	390	
Sequential ($\|i-j\| = 1$)	322	
Medium range ($1 < \|i - j\| < 5$)	122	
Long range ($\|i - j\| \geq 5$)	568	
Dihedral angle constraints	153	
Hydrogen bond constraints	56	
No. of constraints per residue	18.3	
No. of long range constraints per residue	7.0	
Residual constraint violations[c]		
Average No. of distance violations per structure		
0.1–0.2 Å	3.60	
0.2–0.5 Å	0.05	
>0.5 Å	0	
Average No. of dihedral angle violations per structure		
1–10°	12.55	
>10°	0	
Model quality[c]		
RMSD backbone atoms (Å)[d]	0.5	
RMSD heavy atoms (Å)[d]	1.0	
RMSD bond lengths (Å)	0.018	
RMSD bond angles (°)	1.2	
MolProbity Ramachandran statistics[c,d]		
Most favored regions (%)	97.0	
Allowed regions (%)	3.0	
Disallowed regions (%)	0	
Global quality scores (raw/*Z*-score)[c]		
Verify3D	0.39	−1.12
Prosall	0.47	−0.74
Procheck (phi–psi)[d]	−0.56	−1.89
Procheck (all) [d]	−0.26	−1.54
MolProbity clash	15.13	−1.07
RPF scores[e]		
Recall/precision	0.96	0.87
F-measure/DP-score	0.92	0.78
BMRB accession code	6173	
PDB accession code[f]	2LP6	

[a]Structural statistics computed for the ensemble of 20 deposited structures.
[b]Computed using AVS software[16] from the expected number of peaks, excluding: highly exchangeable protons (N-terminal and Lys amino and Arg guanido groups, hydroxyls of Ser, Thr, Tyr), carboxyls of Asp and Glu, nonprotonated aromatic carbons, and the C-terminal 6-His tag.
[c]Calculated using PSVS 1.4[28]. Average distance violations were calculated using the sum over r^{-6}.
[d]Based on ordered residue ranges [S(phi) + S(psi) > 1.8], 2-12,21-76,79-87.
[e]RPF scores as defined by Huang et al.[29].
[f]PDB ID 2LP6 is a refined structure replacing PDB ID 1SQR.

RNA, in the extra-ribosomal functions of RP-L35Ae, and/or in stabilizing the RP-L35Ae fold.

The structural similarities between RP-L35Ae and eEF-1A are also noteworthy because both proteins appear to function outside of the ribosome as modulators of apoptosis. While RP-L35Ae inhibits apoptosis[4,5], the larger EF-Tu/eEF-1A protein has two isoforms that differ in their effect on apoptosis. Expression of eEF-1A-1 is associated with increased apoptosis while expression of eEF-1A-2 is associated with decreased apoptosis.[38] The similarity revealed between the RP-L35Ae structure and the β-barrel domains found in both isoforms of eEF-1A suggests that RP-L35Ae, eEF-1A-1 and eEF-1A-2 modulate apoptosis via interaction with a common target protein or set of target proteins and that the β-barrel domains in eEF-1A isoforms play a critical role in the mechanism by which eEF-1A isoforms modulate apoptosis.

Subsequent to releasing the *P. furiosus* RP-L35Ae structure in the PDB, the 80S eukaryotic ribosomes from *Triticum aestivum* and *Saccharomyces cerevisiae* were determined by cryoelectron microscopy (cryo-EM).[39,40] Using our structure of RP-L35Ae, the L35Ae subunit of *T. aestivum* and the homologous rpl33 subunit of *S. cerevisiae* were located and modeled to 5.5 and 6.1 Å resolution, respectively. These models, apparently based in part on the released coordinates of L35Ae, are shown in Figure 1(g). Many of the *T. aestivum* subunits, including L35Ae, were modeled using the corresponding protein sequences for the related *Oryza sativa* homolog due to lack of complete sequence information for the *T. aestivum* genome.[40] The *P. furiosus* protein has 86% sequence identity to both the *T. aestivum*/*O. sativa* and *S. cerevisiae* proteins [Fig. 1(a)]. The location of the L35Ae protein within the context of the large subunit of each eukaryotic ribosome confirms our hypotheses for the RNA and protein binding interfaces of the *P. furiosus* protein [Fig. 1(g)]. In particular, the tRNA binding surface is unoccupied in the tRNA-free ribosome structure [Fig. 1(g)]. Interestingly, a crystal structure of the *S. cerevisiae* 80S ribosome[41] reported at the same time lacked the homologous rpl33 subunit. Superposition of the two yeast ribosomes show that there is an empty space in the crystal structure corresponding to the position of rpl33 in the cryo-EM model. However, the neighboring L6E homolog also appears to be missing from this crystal structure. These observations suggest that the lack of the RP-L35Ae homolog in the *S. cerevisiae* crystal structure could be a result of purification and crystallization processes.

The solution NMR structure reported here reveals that the tRNA binding RP-L35Ae family, which based on sequence information alone does not appear homologous to any other protein family, adopts a well-studied tRNA binding fold. This structure has allowed identification of a putative tRNA binding site on the RP-L35Ae surface and for inference of homology between the RP-L35Ae family and other tRNA binding proteins. Subsequent to this structure determination, putative RNA, and protein-binding sites were confirmed when L35Ae homologs were modeled in cryo-EM structures of *T. aestivum* and *S. cerevisiae* ribosomes.[39,40] Further exploration of the RP-L35Ae structure and its biochemistry may reveal additional information about ribosomal evolution, as well as its proposed extra-ribosomal functions in cancer pathology and drug resistance.

ACKNOWLEDGMENTS

The authors thank A. Bhattacharya, J. Everett, M. Gerstein, C.S. Goh, G.V.T. Swapna, and H. Moseley for technical assistance and helpful discussions. A portion of the NMR spectra were acquired in the Environmental Molecular Sciences Laboratory (EMSL), a national scientific user facility sponsored by the Department of Energy's Office of Biological and Environmental Research and located at Pacific Northwest National Laboratory, Richland, WA.

REFERENCES

1. Schmeing TM, Ramakrishnan V. What recent ribosome structures have revealed about the mechanism of translation. Nature 2009;461:1234–1242.
2. Marion MJ, Marion C. Localization of ribosomal proteins on the surface of mammalian 60S ribosomal subunits by means of immobilized enzymes. Correlation with chemical cross-linking data. Biochem Biophys Res Commun 1987;149:1077–1083.
3. Ulbrich N, Wool IG, Ackerman E, Sigler PB. The identification by affinity chromatography of the rat liver ribosomal proteins that bind to elongator and initiator transfer ribonucleic acids. J Biol Chem 1980;255:7010–7019.
4. Lopez CD, Martinovsky G, Naumovski L. Inhibition of cell death by ribosomal protein L35a. Cancer Lett 2002;180:195–202.
5. Kasai H, Nadano D, Hidaka E, Higuchi K, Kawakubo M, Sato TA, Nakayama J. Differential expression of ribosomal proteins in human normal and neoplastic colorectum. J Histochem Cytochem 2003;51:567–574.
6. Warner JR, McIntosh KB. How common are extraribosomal functions of ribosomal proteins? Mol Cell 2009;34:3–11.
7. Finn RD, Mistry J, Tate J, Coggill P, Heger A, Pollington JE, Gavin OL, Gunasekaran P, Ceric G, Forslund K, Holm L, Sonnhammer EL, Eddy SR, Bateman A. The Pfam protein families database. Nucleic Acids Res 2010;38:D211–D222.
8. Ferbitz L, Maier T, Patzelt H, Bukau B, Deuerling E, Ban N. Trigger factor in complex with the ribosome forms a molecular cradle for nascent proteins. Nature 2004;431:590–596.
9. Lecompte O, Ripp R, Thierry JC, Moras D, Poch O. Comparative analysis of ribosomal proteins in complete genomes: an example of reductive evolution at the domain scale. Nucleic Acids Res 2002;30:5382–5390.
10. Acton TB, Xiao R, Anderson S, Aramini J, Buchwald WA, Ciccosanti C, Conover K, Everett J, Hamilton K, Huang YJ, Janjua H, Kornhaber G, Lau J, Lee DY, Liu G, Maglaqui M, Ma L, Mao L, Patel D, Rossi P, Sahdev S, Shastry R, Swapna GV, Tang Y, Tong S, Wang D, Wang H, Zhao L, Montelione GT. Preparation of protein samples for NMR structure, function, and small-molecule screening studies. Methods Enzymol 2011;493:21–60.
11. Jansson M, Li YC, Jendeberg L, Anderson S, Montelione GT, Nilsson B. High-level production of uniformly ^{15}N- and ^{13}C-enriched fusion proteins in *Escherichia coli*. J Biomol NMR 1996;7:131–141.
12. Delaglio F, Grzesiek S, Vuister GW, Zhu G, Pfeifer J, Bax A. NMRPipe: a multidimensional spectral processing system based on UNIX pipes. J Biomol NMR 1995;6:277–293.

13. Goddard TD, Kneller DG. SPARKY 3: University of California, San Francisco. See also: http://www.cgl.ucsf.edu/home/sparky/.
14. Moseley HN, Monleon D, Montelione GT. Automatic determination of protein backbone resonance assignments from triple resonance nuclear magnetic resonance data. Methods Enzymol 2001;339:91–108.
15. Neri D, Szyperski T, Otting G, Senn H, Wüthrich K. Stereospecific nuclear magnetic resonance assignments of the methyl groups of valine and leucine in the DNA-binding domain of the 434 repressor by biosynthetically directed fractional ^{13}C labeling. Biochemistry 1989;28:7510–7516.
16. Moseley HN, Sahota G, Montelione GT. Assignment validation software suite for the evaluation and presentation of protein resonance assignment data. J Biomol NMR 2004;28:341–355.
17. Vuister GW, Bax A. Quantitative *J* correlation: a new approach for measuring homonuclear three-bond $J(H^NH^\alpha)$ coupling constants in ^{15}N-enriched proteins. J Am Chem Soc 1993;115:7772–7777.
18. Güntert P, Mumenthaler C, Wüthrich K. Torsion angle dynamics for NMR structure calculation with the new program DYANA. J Mol Biol 1997;273:283–298.
19. Herrmann T, Güntert P, Wüthrich K. Protein NMR structure determination with automated NOE assignment using the new software CANDID and the torsion angle dynamics algorithm DYANA. J Mol Biol 2002;319:209–227.
20. Shen Y, Delaglio F, Cornilescu G, Bax A. TALOS+: a hybrid method for predicting protein backbone torsion angles from NMR chemical shifts. J Biomol NMR 2009;44:213–223.
21. Brünger AT, Adams PD, Clore GM, DeLano WL, Gros P, Grosse-Kunstleve RW, Jiang JS, Kuszewski J, Nilges M, Pannu NS, Read RJ, Rice LM, Simonson T, Warren GL. Crystallography & NMR system: a new software suite for macromolecular structure determination. Acta Crystallogr D Biol Crystallogr 1998;54:905–921.
22. Linge JP, Williams MA, Spronk CA, Bonvin AM, Nilges M. Refinement of protein structures in explicit solvent. Proteins 2003;50:496–506.
23. Lovell SC, Davis IW, Arendall WB, 3rd, de Bakker PI, Word JM, Prisant MG, Richardson JS, Richardson DC. Structure validation by Cα geometry: ϕ,ψ and Cβ deviation. Proteins 2003;50:437–450.
24. Davis IW, Leaver-Fay A, Chen VB, Block JN, Kapral GJ, Wang X, Murray LW, Arendall WB, 3rd, Snoeyink J, Richardson JS, Richardson DC. MolProbity: all-atom contacts and structure validation for proteins and nucleic acids. Nucleic Acids Res 2007;35:W375–W383.
25. Laskowski RA, MacArthur MW, Moss DS, Thornton JM. PROCHECK: a program to check the stereochemical quality of protein structures. J Appl Crystallogr 1993;26:283–291.
26. Lüthy R, Bowie JU, Eisenberg D. Assessment of protein models with three-dimensional profiles. Nature 1992;356:83–85.
27. Sippl MJ. Recognition of errors in three-dimensional structures of proteins. Proteins 1993;17:355–362.
28. Bhattacharya A, Tejero R, Montelione GT. Evaluating protein structures determined by structural genomics consortia. Proteins 2007;66:778–795.
29. Huang YJ, Powers R, Montelione GT. Protein NMR recall, precision, and F-measure scores (RPF scores): structure quality assessment measures based on information retrieval statistics. J Am Chem Soc 2005;127:1665–1674.
30. Huang YJ, Tejero R, Powers R, Montelione GT. A topology-constrained distance network algorithm for protein structure determination from NOESY data. Proteins 2006;62:587–603.
31. Baker NA, Sept D, Joseph S, Holst MJ, McCammon JA. Electrostatics of nanosystems: application to microtubules and the ribosome. Proc Natl Acad Sci USA 2001;98:10037–10041.
32. Glaser F, Pupko T, Paz I, Bell RE, Bechor-Shental D, Martz E, Ben-Tal N. ConSurf: identification of functional regions in proteins by surface-mapping of phylogenetic information. Bioinformatics 2003;19:163–164.
33. Falquet L, Pagni M, Bucher P, Hulo N, Sigrist CJ, Hofmann K, Bairoch A. The PROSITE database, its status in 2002. Nucleic Acids Res 2002;30:235–238.
34. Murzin AG, Brenner SE, Hubbard T, Chothia C. SCOP: a structural classification of proteins database for the investigation of sequences and structures. J Mol Biol 1995;247:536–540.
35. Orengo CA, Michie AD, Jones S, Jones DT, Swindells MB, Thornton JM. CATH – hierarchic classification of protein domain structures. Structure 1997;5:1093–1108.
36. Voorhees RM, Schmeing TM, Kelley AC, Ramakrishnan V. The mechanism for activation of GTP hydrolysis on the ribosome. Science 2010;330:835–838.
37. Rashid R, Liang B, Baker DL, Youssef OA, He Y, Phipps K, Terns RM, Terns MP, Li H. Crystal structure of a Cbf5-Nop10-Gar1 complex and implications in RNA-guided pseudouridylation and dyskeratosis congenita. Mol Cell 2006;21:249–260.
38. Mateyak MK, Kinzy TG. eEF1A: thinking outside the ribosome. J Biol Chem 2010;285:21209–21213.
39. Armache JP, Jarasch A, Anger AM, Villa E, Becker T, Bhushan S, Jossinet F, Habeck M, Dindar G, Franckenberg S, Marquez V, Mielke T, Thomm M, Berninghausen O, Beatrix B, Söding J, Westhof E, Wilson DN, Beckmann R. Cryo-EM structure and rRNA model of a translating eukaryotic 80S ribosome at 5.5-Å resolution. Proc Natl Acad Sci USA 2010;107:19748–19753.
40. Armache JP, Jarasch A, Anger AM, Villa E, Becker T, Bhushan S, Jossinet F, Habeck M, Dindar G, Franckenberg S, Marquez V, Mielke T, Thomm M, Berninghausen O, Beatrix B, Söding J, Westhof E, Wilson DN, Beckmann R. Localization of eukaryote-specific ribosomal proteins in a 5.5-Å cryo-EM map of the 80S eukaryotic ribosome. Proc Natl Acad Sci USA 2010;107:19754–19759.
41. Ben-Shem A, Jenner L, Yusupova G, Yusupov M. Crystal structure of the eukaryotic ribosome. Science 2010;330:1203–1209.
42. Chenna R, Sugawara H, Koike T, Lopez R, Gibson TJ, Higgins DG, Thompson JD. Multiple sequence alignment with the Clustal series of programs. Nucleic Acids Res 2003;31:3497–3500.
43. Duan J, Li L, Lu J, Wang W, Ye K. Structural mechanism of substrate RNA recruitment in H/ACA RNA-guided pseudouridine synthase. Mol Cell 2009;34;427–439.
44. Gouet P, Courcelle E, Stuart DI, Metoz F. ESPript: analysis of multiple sequence alignments in PostScript. Bioinformatics 1999;15:305–308.